Effect of Molecular Weight on Network Formation in Linear ABC Triblock Copolymers

Thomas H. Epps, III† and Frank S. Bates*

Department of Chemical Engineering and Materials Science, University of Minnesota, Minneapolis, Minnesota 55455

Received October 1, 2005; Revised Manuscript Received January 10, 2006

ABSTRACT: A series of linear poly(isoprene-*b*-styrene-*b*-ethylene oxide) (ISO) triblock copolymers were synthesized to investigate the effects of molecular weight and segregation strength on block copolymer network phases. Analysis of small-angle X-ray scattering (SAXS), dynamic mechanical spectroscopy (DMS), and transmission electron microscopy (TEM) data shows that several factors influence network formation. Increasing the polymer molecular weight 50−100% above the value necessary to place the order−disorder transition temperature within an experimentally accessible range leads to disruption of long-range order at compositions associated with the orthorhombic O^{70} phase in freeze-dried and annealed specimens. Comparable molecular weight three-domain lamellae (LAM_3) behave differently, exhibiting well-ordered morphologies that closely resemble the correlated layers found in diblock copolymers. These findings are interpreted on the basis of the reduction in molecular diffusion that accompanies increasing molecular weight and segregation strength, bridging across the poly(styrene) middle block, and differences in domain topology. These kinetic restrictions can inhibit establishment of equilibrium phase behavior in ABC triblock copolymers but do not necessarily eliminate formation of multifunctional triply periodic materials.

I. Introduction

Block copolymer self-assembly offers exciting possibilities for designing materials endowed with multiple three-dimensionally continuous nanoscale domains. Such network morphologies should find applications as membranes due to a combination of short diffusion path lengths and independent control over porosity, mechanical stability, solvent resistance, and other physical properties. However, the design rules governing network formation are not well established. Parameters that influence phase formation in block copolymer melts include molecular architecture (linear vs branched), number of blocks, degree of polymerization, composition, block statistical segment lengths, and interaction parameters.[1−23] All these variables have been investigated in two-monomer AB diblocks[1−7] and some higher order (A_mB_n) multiblock copolymers;[8−11] several studies have dealt with a few of these parameters in linear ABC triblocks.[12−19,22−29]

Segregation strength, captured in diblocks by the product of the binary interaction parameter χ and the degree of polymerization N,[2,5−7] is fundamentally important to all classes of block copolymers. Increasing χN above the condition for microphase separation (within mean-field theory this occurs at $(\chi N)_{ODT} = 10.5$ for compositionally symmetric diblocks)[30] leads to ordered phases, including the double-gyroid network structure. Several groups have probed the effects of varying segregation strength and/or molecular weight on the stability of the double gyroid in diblock copolymers,[2,5−7] but these parameters have not been evaluated in detail with network forming "three-color" (i.e., three-domain) triblock copolymers.

Two asymptotic segregation limits can be identified in block copolymers:[31] the strong segregation limit (SSL, $\chi N \geq 100$ in diblocks) and the weak segregation limit (WSL, $\chi N < \sim 10$ in diblocks). The SSL is characterized by sharp domain boundaries and limited mixing of chemically distinct blocks. These conditions produce extended (stretched) chain conformations, an inescapable consequence of localizing the block junctions at narrow interfaces while maintaining uniform density. Chain stretching is manifested through the molecular weight dependence of the domain spacing: $d \sim N^{2/3}\chi^{1/6}$.[31] In the WSL the blocks mix intimately at lower χN as evidenced by correlation hole scattering that scales as $d \sim N^{1/2}$. As χN increases toward $(\chi N)_{ODT}$, finite amplitude composition fluctuations develop, ultimately inducing a transition from disorder to order. Between approximately $\chi N \approx 10$ and $\chi N \approx 100$, an intermediate segregation regime (ISR) exists, characterized by a composition profile that evolves from sinusoidal (near $(\chi N)_{ODT}$) to nearly pure domains separated by a finite interfacial thickness that narrows as the SSL is approached.

Morphological changes, especially those involving network phases, have been reported in the ISR. For example, Khandpur et al.[2] reported that the double gyroid is extinguished, in favor of cylindrical and lamellar states, when χN approaches the SSL in PS−PI diblock copolymers. This result is substantiated by self-consistent mean-field calculations described by Matsen.[7] Other groups have found behavior consistent with the above results.[3,5,32] However, Davidock et al.[6] recently found the gyroid phase in strongly segregated partially fluorinated diblock copolymers, and Burger et al.[33] reported a perforated lamellar phase in another fluorinated diblock copolymer. Thus, the limit of network stability as a function of segregation strength remains an open question for diblocks and virtually unexplored with higher order multiblocks.

We recently identified a composition channel in a series of linear poly(isoprene-*b*-styrene-*b*-ethylene oxide) (ISO) triblock copolymer melts that contains three different network phases: Q^{230} (core−shell double gyroid), O^{70} (orthorhombic network), and Q^{214} (alternating gyroid).[18,29] This network phase region presents an excellent opportunity for exploring the role of segregation strength (through changes in the degree of polymerization) in "three-color" networks. Because the ISO system

† Current address: NIST−Polymers Division, 100 Bureau Drive, MS 8542, Gaithersburg, MD 20899-8542.

* To whom correspondence should be addressed.

10.1021/ma052132o CCC: $33.50
Published on Web 03/14/2006

Table 1. Higher Molecular Weight Polymers

polymer[a]	M_n (Da)	M_w/M_n	f_I[a]	f_S[a]	f_O[a]	phase[b]
IS-3[c]	17 500	1.04	0.47	0.53	0.00	LAM_2
ISO-3a	19 300	1.08	0.44	0.48	0.08	LAM_2
ISO-3c	21 200	1.06	0.39	0.44	0.17	O^{70}
ISO-3b	22 200	1.07	0.37	0.41	0.22	LAM_3
IS-4	23 800	1.02	0.47	0.53	0.00	LAM_2
ISO-4a	28 700	1.07	0.40	0.45	0.15	O^{70}
ISO-4b	31 200	1.07	0.36	0.40	0.24	LAM_3
IS-7	25 000	1.05	0.51	0.49	0.00	LAM_2
ISO-7a	30 000	1.05	0.44	0.40	0.16	network
ISO-7b	30 700	1.06	0.41	0.39	0.20	network
IS-13	30 900	1.04	0.50	0.50	0.00	LAM_2
ISO-13a	35 500	1.04	0.45	0.46	0.09	LAM_2
ISO-13b	36 800	1.05	0.44	0.42	0.14	network
ISO-13c	37 700	1.06	0.42	0.39	0.19	network
ISO-13d	39 200	1.07	0.40	0.38	0.22	LAM_3
ISO-13e	43 000	1.09	0.36	0.33	0.31	LAM_3

[a] Volume fractions calculated from homopolymer densities at 140 °C ($\rho_I = 0.830$, $\rho_S = 0.969$, $\rho_O = 1.064$ g/mol).[37] [b] "Network" represents an unidentified, poorly ordered, triply periodic material. [c] The IS-3 diblock copolymer in this work differs from the IS-3 diblock copolymer in ref 18.

is nearly symmetric over the experimental temperature range, $\chi_{IS} \approx \chi_{SO} < \chi_{IO}$,[34] segregation strength is relatively balanced across both interfacial surfaces. This symmetry of interaction parameters is similar to that found in the poly(isoprene-*b*-styrene-*b*-2-vinylpyridine) (ISV) system studied by Mogi et al., where morphologies including the alternating gyroid also were reported.[13,35] In both the ISO and ISV systems, increasing the overall degree of polymerization, *N*, will almost uniformly increase the segregation strength, analogous to the situation encountered with the diblock-based gyroid phase. (Doping the O domains in the ISO and SIO triblock systems with lithium salts has been shown to disrupt this segregation strength symmetry, resulting in elimination of the network phases.[17,36])

In this report we describe a series of experiments using ISO triblocks prepared at compositions associated with network phase formation and with molecular weights up to twice those reported previously. A combination of techniques, including small-angle X-ray scattering (SAXS), dynamic mechanical spectroscopy (DMS), and transmission electron microscopy (TEM), was employed to probe the resulting phase behavior.

II. Experimental Section

Synthesis and Characterization of ISO Triblock Copolymers. ISO triblock copolymers were synthesized using sequential anionic polymerization techniques described elsewhere.[16] The triblock copolymer/THF solution was concentrated using a rotary evaporator and dissolved in dichloromethane. Residual salts were removed by repeated washings with a sodium bicarbonate saturated water solution. Acid removal was monitored by measuring the pH of the water and was considered complete when the distilled water following washing was pH = 7. The dichloromethane was removed using a rotary evaporator, and the purified triblock was freeze-dried in a benzene/THF mixture (95 vol % benzene) until the vacuum level reached baseline values.

Copolymer molar compositions were determined by ^{1}H NMR and converted to volume fractions using published homopolymer densities at 140 °C (see Table 1).[37] Molecular weight distributions and polydispersities were determined by size exclusion chromatography (SEC) using Phenomenex Phenogel columns coupled to a Wyatt Dawn DSP laser photometer and a Wyatt differential refractometer. A more complete description of these characterization methods is found in ref 15.

Sample Preparation. Block copolymer samples were mixed in 10 mL vials with either benzene, *n*-hexane, or THF and stirred for 24 h. Samples were then freeze-dried to constant weight, where periodic immersion in liquid nitrogen kept the *n*-hexane and THF mixtures frozen. These three solvents survey a range of solubility parameters ($\delta = 7.3$ (*n*-hexane), 9.1 (THF), and 9.2 (benzene) [cal/cm^3]$^{1/2}$),[38] and they were used to examine the influence of the freeze-drying solvent on the resulting block copolymer morphology.

IT Small-Angle X-ray Scattering (IT-SAXS). IT-SAXS experiments were conducted at the University of Minnesota Institute of Technology (IT) characterization facility. 2D-SAXS data were collected on a Siemens HI-STAR multiwire area detector at a sample-to-detector distance of 230 cm. 1.54 Å Cu Kα X-rays were generated using a Rigaku RU-200BVH rotating anode equipped with a microfocus cathode, a nickel foil filter, and total reflecting Franks mirror optics. Specimens were heated to 200 °C and annealed for 10−12 h prior to data collection.

APS-SAXS (Synchrotron). Synchrotron SAXS experiments were conducted on the DND-CAT at the Advanced Photon Source (Argonne National Laboratory) using $\lambda = 0.827$ Å wavelength X-rays. The sample-to-detector distance was 501 cm, and data were acquired with a Mar CCD area detector. Sample temperature was controlled on a liquid nitrogen-cooled DSC maintained under a helium purge. ISO specimens were annealed for 2−3 h at 200 °C before being transported to Argonne National Labs. At the APS beamline samples were heated to 200 °C and held for 15 min prior to data collection at 160 °C.

Dynamic Mechanical Spectroscopy (DMS). Mechanical spectroscopy experiments were conducted on a Rheometrics Scientific ARES strain-controlled rheometer under a nitrogen atmosphere using 25 mm diameter parallel plates. Dynamic elastic (G') and loss (G'') moduli were recorded at frequencies between 0.1 and 100 rad/s at various temperatures. Data were acquired in 10 °C decrements while cooling from 230 °C (210 °C for sample ISO-3c). In all cases the strain amplitude was 1%, which was within the linear viscoelastic regime. Isothermal temperature sweeps also were run at a 1% strain amplitude and 1 °C/min heating/cooling rate. All samples had T_{ODT}'s above 210 °C, except IS-3 [140 °C], ISO-3a [207 °C], and IS-4 [187 °C], which were all two-domain lamellar structures.

Transmission Electron Microscopy (TEM). TEM micrographs were collected on a JEOL 1210 TEM operating at 120 kV in the IT Characterization Facility. Samples (50−100 nm thickness) were prepared with a Reichart ultramicrotome using a Microstar diamond knife operated at −75 to −90 °C. Electron scattering contrast was obtained by exposing the sliced ISO specimens to a 4% aqueous OsO_4 solution vapor for ∼5 min. This oxidizing agent reacts preferentially with the poly(isoprene) blocks. All TEM images reported here were obtained from samples also characterized by SAXS, affording a direct comparison of real and reciprocal space data. Previous studies have shown that O-block crystallization has a minimal effect on the overall block copolymer microstructures examined at ambient conditions (TEM) and elevated temperatures (SAXS),[18,29] and the effect was not explored further in this work.

III. Results and Analysis

Previous investigations of ISO phase behavior have focused on polymers in the vicinity of T_{ODT}.[16,18,29,39] The current investigation examines the composition window associated with the network phases at higher segregation strengths, accessed by increasing the triblock molecular weight. For comparative purposes the I/S/O phase prism is illustrated on the left side of Figure 1, with a colored rectangle highlighting the $f_S = f_I$ isopleth. The experimental PS−PI phase diagram, described by Khandpur et al.,[2] is shown on the PS−PI diblock face of the prism. No single definition characterizes segregation strength with ABC triblocks since there are three independent χ_{ij} parameters. For convenience, and because the ISO system is nearly energetically symmetric ($\chi_{IS} \approx \chi_{SO} < \chi_{IO}$), we shall overlook this point throughout this article. Two-domain and three-domain lamellar regions, and a channel of three-domain network phases (Q^{230}, O^{70}, and Q^{214}), were established previously using ISO specimens located near the order−disorder

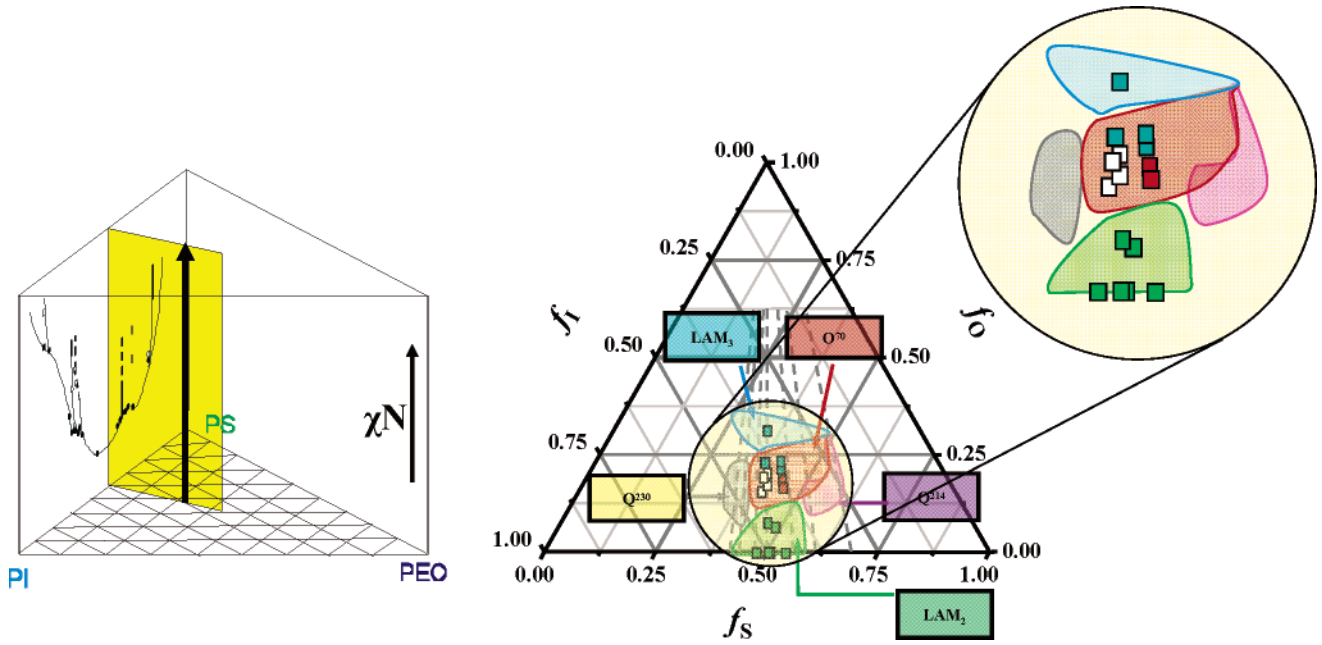

Figure 1. The left panel shows the I/S/O phase prism, where the focus region for the higher molecular weight studies is indicated by the colored rectangle. The experimental PS−PI phase diagram[2] is displayed on the I/S face. The right panel shows the poly(isoprene-*b*-styrene-*b*-ethylene oxide) (ISO) volume fraction phase portrait. Shaded regions highlight the neat triblock locations for three network phases, Q^{230}, O^{70}, and Q^{214}, and the two-domain (LAM_2) and three-domain (LAM_3) lamellar materials as determined by previous studies on samples near their ODT.[18,29] Higher molecular weight sample locations are indicated by colored squares, where the color corresponds to the sample morphology (see magnified region) (blue, LAM_3; green, LAM_2; red, O^{70}; white, network). Dashed lines represent isopleths examined in previous ISO lower molecular weight studies.[18,29]

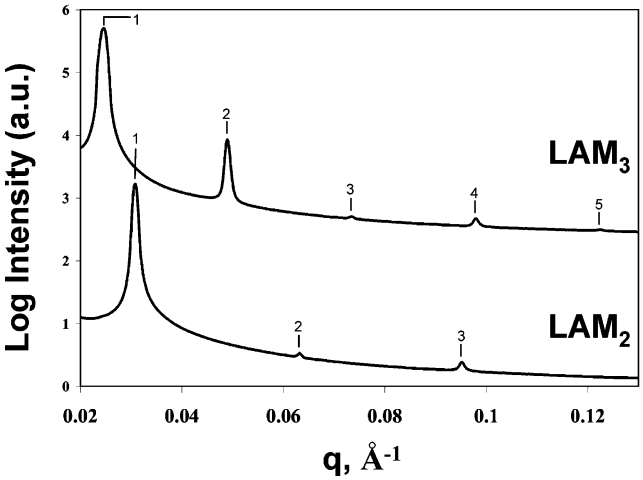

Figure 2. Synchrotron SAXS data for ISO-13d, a LAM_3 material (upper curve), and ISO-13a, a LAM_2 polymer (lower curve). Samples were prepared by annealing at 200 °C followed by annealing and measurement at 160 °C. The integer moduli values are indicative of lamellar morphologies for both curves.

transition temperature (T_{ODT}), as identified in Figure 1, right panel. Specimens considered in this work (Table 1) are located by the point symbols in the triangular phase portrait.

Lamellar Phases. SAXS patterns obtained at 160 °C from two specimens, ISO-13a ($f_O \cong 0.09$) and ISO-13d ($f_O \cong 0.22$), located on the ISO-13 isopleth, are shown in Figure 2. Bragg peaks appear at q^*, $2q^*$, and $3q^*$ for ISO-13a and at q^*, $2q^*$, $3q^*$, $4q^*$, and $5q^*$ for ISO-13d (q^* represents the primary peak position). These sharp diffraction peaks are indicative of significant long-range order. On the basis of the relative q-spacings and peak intensities, we conclude that these symmetric triblocks contain two-domain (LAM_2) and three-domain (LAM_3) lamellar morphologies, respectively. The relative intensities of the second-order peak in the LAM_2 sample and the third-order peak in the LAM_3 sample are expected for the ISO system, as explained in previous work.[18] Here we note that LAM_2 refers to ordered lamellae on the O-lean side of the network window. The LAM_2 phase contains domains rich in I and others rich in S mixed with a minor amount of O. The distinction between two and three domains is somewhat arbitrary, especially under conditions where a continuous composition path exists from diblock to symmetric triblock copolymers.[40] However, the network channel identified in the ISO system clearly separates these two limits into well-defined states.

TEM micrographs (Figure 3) obtained from thin sections of ISO-13a and ISO-13d, stained with OsO_4, support these lamellar assignments. Dark stripes in these images correspond to I domains, while light stripes account for unstained S and/or O domains. Both materials display considerable translational order, consistent with the SAXS diffraction patterns.

The results shown in Figures 2 and 3 are nearly indistinguishable from SAXS and TEM data obtained in lower molecular weight ISO experiments, leading us to conclude that doubling the molecular weight of these triblock copolymer materials does not inhibit the development of long-range translational lamellar order, analogous to the behavior of two-monomer block copolymer melts.

Network Phases. Synchrotron SAXS powder patterns obtained at 160 °C from several samples with intermediate poly(ethylene oxide) compositions ($0.15 \leq f_O \leq 0.19$) are shown in Figure 4. These materials lie within the O^{70} composition window defined by our previous ISO studies,[18,29] with molecular weights ranging from 21 to 38 kg/mol. The scattering pattern from the lowest molecular weight sample (ISO-3c, 21 kg/mol) contains clearly delineated (although not instrument resolution limited) Bragg peaks that form a "fingerprint" shown elsewhere to be associated with the *Fddd* (#70) space group;[16,18,39] the pattern is indexed accordingly in Figure 4. Increasing the molecular weight to 29 kg/mol, at roughly the same composition (ISO-4a), results in several modifications to the SAXS pattern. The leading order

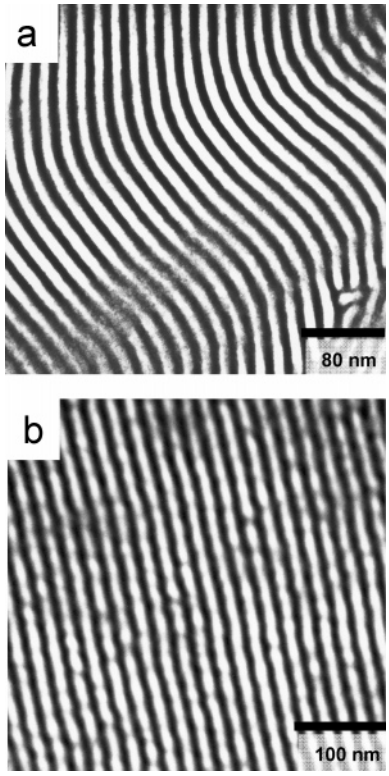

Figure 3. (a) TEM micrograph from ISO-13a, representative of two-domain lamellar structures. (b) TEM micrograph from ISO-13d, representative of three-domain lamellar structures. Dark regions in TEM micrographs result from OsO_4 staining of the poly(isoprene) domains. The unstained S and O domains appear lighter.

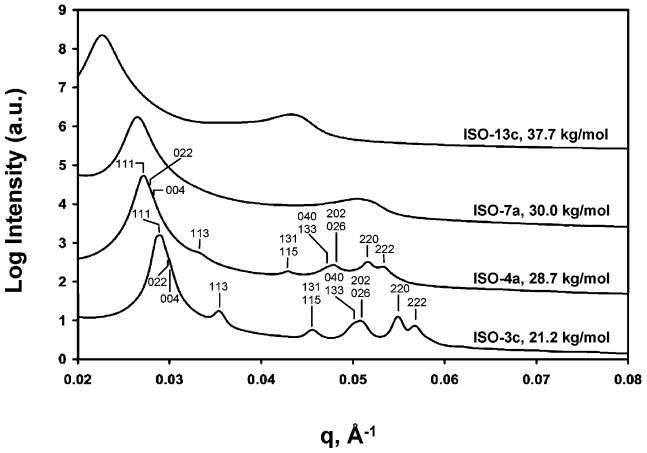

Figure 4. APS-SAXS data (160 °C) for several network materials freeze-dried from benzene: ISO-3c ($f_O = 0.17$), ISO-4a ($f_O = 0.15$), ISO-7a ($f_O = 0.16$), and ISO-13c ($f_O = 0.19$). Peak locations for ISO-3c and 4a are consistent with the *Fddd* space group. All samples were heated to 200 °C and annealed prior to data collection.

peak broadens and shifts to lower q, and the higher order peaks decrease in intensity and resolution. Nevertheless, the *Fddd* "fingerprint" is still identifiable.

The SAXS responses from the two highest molecular weight specimens (ISO-7a and ISO-13c) are qualitatively different. Only two broad reflections are evident, located at relative positions q^* and $1.92q^*$. Annealing these samples at 130 °C (i.e., well above the poly(styrene) glass transition) for 30 days in vacuum-sealed ampules did not appreciably change the SAXS response. It is tempting to conclude that these results signal a transition to poorly organized lamellae. As shown below, this is not the case.

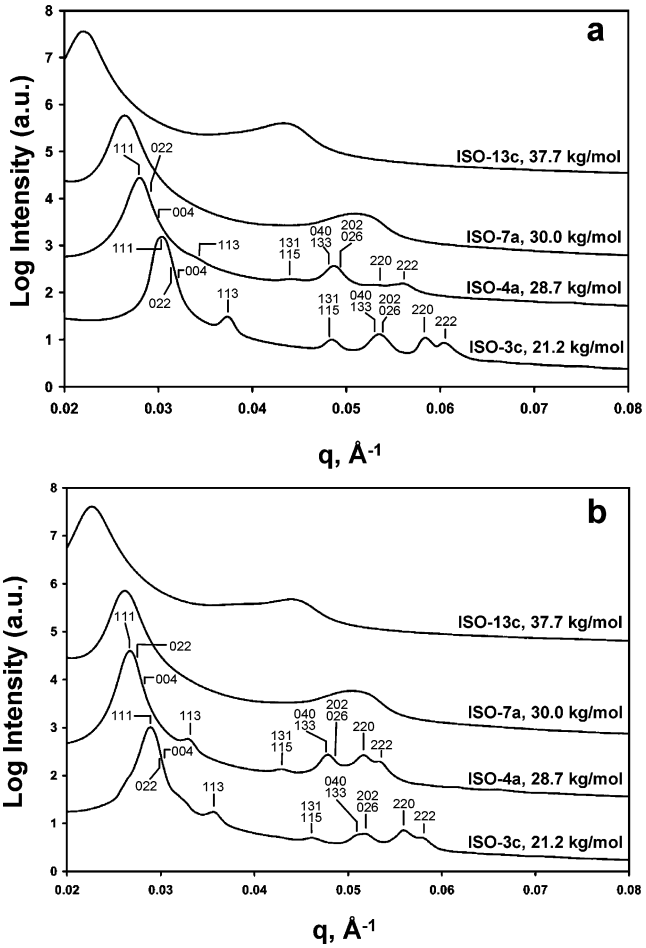

Figure 5. (a) APS-SAXS data (160 °C) for several network materials freeze-dried from *n*-hexane: ISO-3c, ISO-4a, ISO-7a, and ISO-13c. **(**b**)** APS-SAXS data for same samples as in (a), except freeze-dried from THF. Peak locations for ISO-3c and 4a are consistent with the *Fddd* space group. All samples were heated to 200 °C and annealed prior to data collection. See Table 1 for sample compositions.

Identical SAXS experiments were conducted after two additional sample preparation procedures. Each of the four triblock copolymers was freeze-dried from *n*-hexane (Figure 5a) and THF (Figure 5b) mixtures. Along with benzene, these three solvents survey a range of solubility parameters ($\delta = 7.3$ (*n*-hexane), 9.1 (THF), and 9.2 (benzene) $[\text{cal/cm}^3]^{1/2}$),[38] and each interacts differently with the three blocks in the ISO materials. Solvent effects on morphology are well-documented in the block copolymer literature.[41−46] In this work, THF and *n*-hexane experiments were employed to address the possibility that the transitions in the benzene SAXS patterns were a consequence of specific interactions with individual blocks. The results shown in Figure 5 indicate this is not the case. (Here we note that freeze-drying from selective solvents is not likely to have as pronounced an effect as the solvent casting methods described by others.[41−46]) With minor exceptions, all three solvent preparations, followed by heat treatments, produced similar results.

Isothermal DMS experiments, conducted as a function of frequency, were used to further probe the properties of the ISO specimens with increasing molecular weight. Figure 6 displays time−temperature superposed $G'(\omega)$ and $G''(\omega)$ measurements obtained from ISO-3c (a), ISO-4a (b), ISO-7a (c), and ISO-13c (d). The $G'(\omega)$ plateau in each panel is consistent with solid-like behavior over a wide range of time scales, a signature of triply periodic structures,[47] and supports a network-like structural

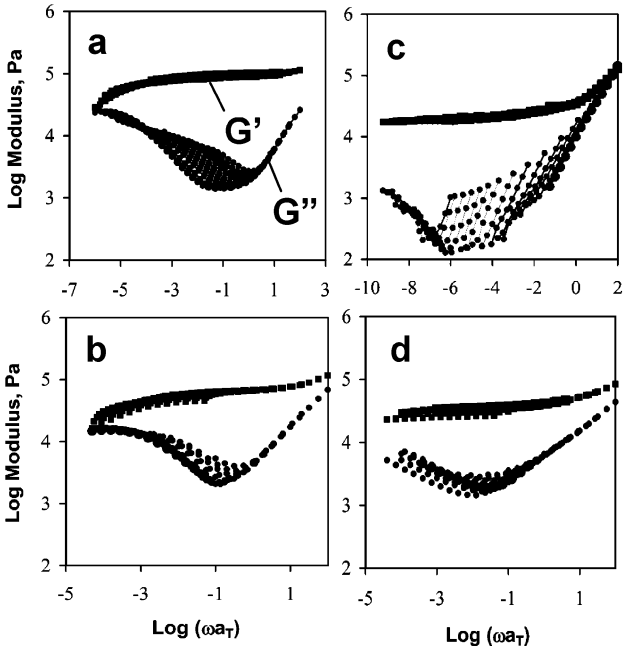

Figure 6. DMS results for higher molecular weight samples. TTS-shifted isothermal frequency sweep data are shown, and G' (upper) and G'' (lower) curves are presented in each case. $T_{ref} = 110$ °C for all samples, and all sweeps were performed in 10 °C decrements. (a) ISO-3c frequency sweep on cooling from 210 to 110 °C. (b) ISO-4a frequency sweep on cooling from 230 to 110 °C. (c) ISO-7a frequency sweep on cooling from 230 to 110 °C. (d) ISO-13c frequency sweep on cooling from 230 to 110 °C. The elastic behavior in all panels is consistent with a triply periodic structure.

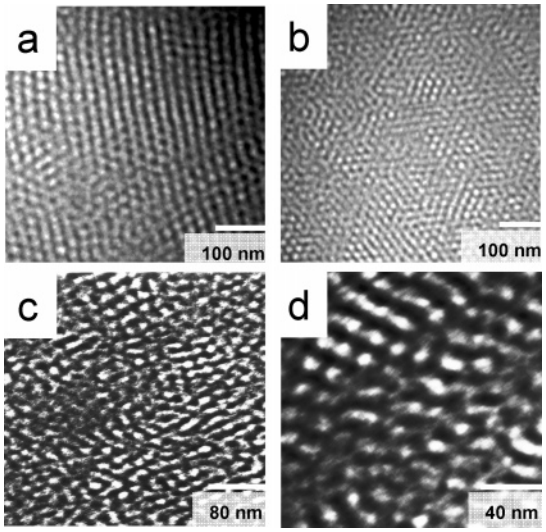

Figure 7. (a) TEM micrograph of ISO-3c ($f_O = 0.17$, $M_n = 21\,200$ g/mol), showing the O^{70} network morphology. (b) TEM micrograph of ISO-4a ($f_O = 0.15$, $M_n = 28\,700$ g/mol), representative of the O^{70} region. **(**c**)** TEM micrograph of ISO-13c ($f_O = 0.19$, $M_n = 37\,700$ g/mol). (d) Higher magnification micrograph of ISO-13c. Dark regions in TEM micrographs result from OsO_4 staining of the I domains, while the unstained S and O domains appear lighter.

assignment for the higher molecular weight materials. This plateau modulus decreases with increasing molecular weight, consistent with the expected trend for three-dimensional periodic microstructures.[47] We interpret this complement of mechanical properties as evidence that all four melt morphologies are characterized by a three-dimensional morphology.

Selected TEM micrographs obtained from three ISO triblocks are shown in Figure 7. Our purpose here is to correlate real-space images, particularly the degree of translational order, with the SAXS patterns described in earlier paragraphs. Figure 7a shows a representative image of ISO-3c (21 200 g/mol). This micrograph resembles those associated with the O^{70} phase in previous publications[16,18,39] and is consistent with the diffraction results found in Figures 4 and 5. Translational order can be traced across the entire image; lower magnification micrographs reveal ordered grains with dimensions in excess of 1 μm. ISO-4a (28 700 g/mol) appears to contain smaller ordered grains (Figure 7b), in agreement with our deductions based on the SAXS results. The state of order changes dramatically with ISO-13c (37 700 g/mol), which appears to be nearly disordered at lower magnification (Figure 7c). A higher magnification image (Figure 7d) reveals a complex morphology with some degree of short-range order. These and other related TEM images rule out a lamellar morphology for sample ISO-13c (and ISO-7a), and we have labeled this morphology "network" in Table 1, although we cannot assign a specific morphology.

IV. Discussion

We initiated the experiments described in this report to explore the feasibility of producing network phases in ABC triblock copolymers at elevated molecular weights and segregation strengths. Two issues are pertinent to this discussion. First, do the network states identified in the ISO system near the ODT persist as molecular weight increases? And second, can these materials achieve high degrees of translational order? Our work provides partial answers to both questions.

The most striking finding of this study is how differently three-domain lamellae (LAM_3) and the O^{70} network phase respond to increasing molecular weight. SAXS patterns (Figure 2) and TEM images (Figure 3) obtained from LAM_3 specimens that approach the SSL exhibit long-range order comparable to that found in the corresponding LAM_2 specimens and other diblock copolymers. In contrast, a modest increase in molecular size, just 50−100% above the value required to place T_{ODT} within experimental range (i.e., ISO-3c vs ISO-7a and ISO-13c), leads to a profound loss of long-range translational order in triblocks located within the O^{70} composition window, even following a month of annealing in the melt state. Although we cannot assign a detailed structure, let alone an ordered symmetry, to the specimens denoted "network" in Table 1, DMS measurements (Figure 6) indicate a three-dimensional elastic structure. TEM images (Figure 7) are consistent with a rather disorganized interconnected morphology.

At first glance, these results appear to differ from publications dealing with strongly segregated AB diblock copolymers, where TEM images illustrate near single crystalline gyroid order, in some cases over length scales spanning many microns.[48] However, we believe these differences reflect a combination of two effects: nearly complete bridging of the central S blocks in the ISO system, thereby coupling translational diffusion along independent I−S and S−O interfaces, and extinction of molecular diffusion perpendicular to domain interfaces (i.e., across domains) as the segregation strength increases.[28] We first consider the lamellar situation.

Molecular diffusion in ordered lamellae can be divided into two contributions, parallel and perpendicular to the domain interfaces. The significance of the latter mode decreases exponentially with molecular weight as demonstrated by the elegant experiments of Lodge and co-workers.[49,50] Regardless of χN, diblock molecules are free to move parallel to the interface, although the time constant is strongly influenced by the state of entanglement. This picture will be applicable to ABC triblocks as well, with an important caveat. Complete domain

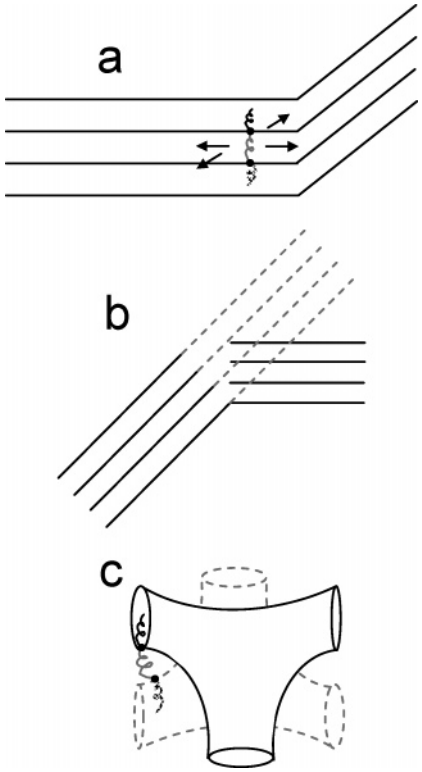

Figure 8. (a) Two-dimensional chain diffusion in lamellar materials. (b) Annealing and improvement of lamellar long-range order, where dashed lines indicated potential location for combination of lamellar grains. (c) Constrained mobility of chains in network structures caused by interfacial curvature.

bridging of the B blocks (required by the chemical connectivity of the copolymer) necessitates the cooperative movement of A−B and B−C block junctions.[28] While we are unaware of any theoretical treatments dealing with this problem, it seems intuitively obvious that parallel diffusion of ABC triblocks will be slower than for AB diblocks, and this effect is likely exacerbated by entanglements. Nevertheless, triblock lamellae can coarsen (see Figure 8a,b) by two-dimensional diffusion, regardless of segregation strength, particularly in the unentangled limit. For the materials considered here (for example ISO-13d), neither the S or I blocks can be considered to be well entangled. (The block entanglement molecular weights are $M_{e,I} = 5429$ g/mol, $M_{e,S} = 13\,309$ g/mol, and $M_{e,O} = 1624$ g/mol.[37])

Network phases and lamellae are fundamentally distinct. While the local state of segregation is only subtly different (e.g., close to zero mean interfacial curvature), a negative interfacial Gauss curvature and the associated saddle surface geometry leads to interpenetrating domains that span three dimensions rather than two. The O^{70}, Q^{230}, and Q^{214} phases are examples of such ordered morphologies, each constructed from closely related trivalent nodes linked together into 10-node loops that tile space according to the indicated space group operations. Though we cannot assign a structure to the disorganized ("network") morphology identified at the higher molecular weights, the combination of the SAXS patterns, DMS results, and TEM images suggests an overall interconnected (e.g., network) topology.

Figure 8c illustrates chain motion in an ABC triblock copolymer network using the alternating gyroid structure. Triblock chains will be configured with A and C end blocks embedded in opposing network domains, separated by bridging B blocks. With perpendicular diffusion arrested, this arrangement makes molecular movement nearly impossible since the

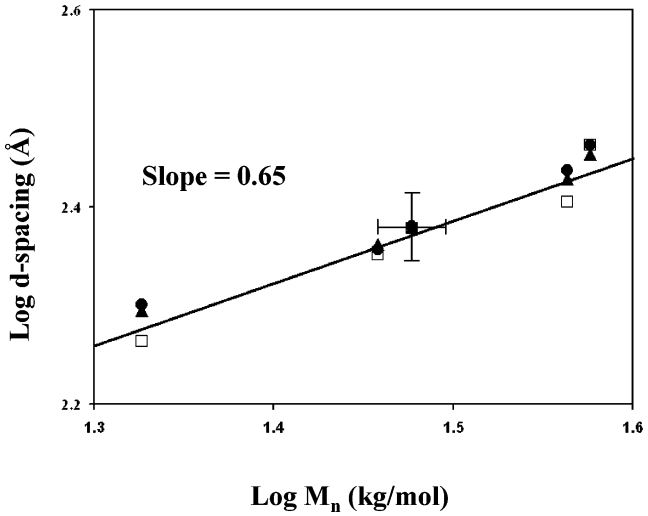

Figure 9. Log−log plot of domain spacing (d spacing) vs molecular weight (M_n) for the samples depicted in Figures 4 and 5. The points lie on a straight line and fit the relationship $d \sim \chi^{1/6}N^{2/3}$, which is expected for strong segregation strength block copolymers. (□) Data from benzene solvent. (▲) Data from *n*-hexane mixture. (●) Data from THF solvent.

A−B and B−C block junctions cannot translate without stretching the B blocks. Careful analysis of the alternating gyroid network topology reveals a highly restricted set of pathways that permit transport of conformationally unperturbed bridged ABC chains. In the absence of domain rupture and re-formation, an unlikely event in the absence of bulk deformation in a strongly segregated state, there is virtually no mechanism for coarsening a disorganized or powdered network morphology. We believe this is the underlying reason why well-formed grains of the O^{70} phase were not identified in the higher molecular weight ISO triblock copolymers.

Our hypothesis regarding the failure to develop long-range order relies on relatively strong segregation, a condition confirmed by the SAXS results in Figures 4 and 5. The domain spacings extracted from the leading order reflections ($d = 2\pi/q^*$) are plotted in logarithmic form vs molecular weight for the triblock copolymers (see Figure 9). A slope of ~0.65 is consistent with that expected in the SSL, $d \sim N^{2/3}$.[4,31,51,52]

Of course, the initial state of order in the ISO network forming materials is established at the point of sample preparation. We purposefully avoided slow solvent casting since this method can induce long-range order as the solution passes through the order−disorder transition during solvent removal. Freeze-drying eliminates this possibility, leading to an initially unstructured morphology. As we have shown here, at higher molecular weights long-range order is not recovered after extensive annealing. However, at lower molecular weights specimens may disorder upon heating with subsequent nucleation and growth of large domains during cooling, as shown in previous work.[18,39] (Grain growth was not studied in the current work because the ceiling temperature of the SAXS instrument [200 °C] was lower than the T_{ODT} of the network materials.)

Finally, we must consider the possibility that ABC triblock network phases are actually extinct at equilibrium in the SSL, as some have suggested with diblocks.[2,3,5] Unfortunately, our experiments do not shed light on this issue. Moreover, we are not optimistic that additional experiments will resolve the question. Given our inability to develop long-range order at $\chi N \cong 50$ (this designation is based on overall N with an average segment mass of 80 g/mol and using $\chi = \chi_{IS} \approx \chi_{SO}$), we believe it is unlikely that freeze-dried specimens will perform better at

yet higher molecular weights. Slow solvent casting may offer a more productive processing method for preparing strongly segregated ISO networks with long-range order, as has been accomplished with diblocks.[48] However, given the results presented here, these morphologies are unlikely to respond to thermal annealing, making a definitive identification of equilibrium phase behavior virtually impossible. Notwithstanding this dilemma, strongly segregated networks will provide useful materials for applications such as membranes and other transport devices. We are currently investigating these issues.

V. Conclusions

This research has shown that molecular weight and segregation strength plays an important role in the development of morphology in ISO triblock copolymers. Increasing the molecular weight to twice that required to place the order−disorder transition temperature within the experimentally accessible range appears to arrest molecular diffusion and consequently prevents the coarsening of interpenetrating network morphologies into coherent ordered grains. Three-domain lamellae do not suffer from this restriction. We attribute this behavior to the combined effects of center block bridging and the extinction of diffusion perpendicular to the interfaces as the segregation strength (χN) increases, restricting the pathways for molecular diffusion.

These findings suggest we will not experimentally establish whether ABC triblock copolymer network phases exist at equilibrium in the strong segregation limit. On the other hand, we can conclude that processing methods leading to materials with triply periodic and multicontinuous network morphologies, such as slow solvent casting, will be remarkably stable. From a practical point of view this would be a very desirable circumstance.

Acknowledgment. This work was supported by the NSF through Grant DMR-0220460 and in part by the Department of Energy through Oak Ridge National Laboratory. The authors thank Ryan Waletzko and Joon Chatterjee for their help synthesizing several of the polymers studied in this work. The authors also thank Eric Cochran for running the *n*-hexane samples at the APS. Use of the Advanced Photon Source at Argonne National Labs was supported by the U.S. Department of Energy, Basic Energy Sciences, Office of Science, under Contract No. W-31-109-Eng-38. This research program has made extensive use of the MRSEC (NSF) supported Institute of Technology Characterization Facility at the University of Minnesota, Twin Cities Campus.

References and Notes

(1) Matsen, M. W.; Schick, M. *Macromolecules* **1994**, *27*, 4014−15.
(2) Khandpur, A. K.; Foerster, S.; Bates, F. S.; Hamley, I. W.; Ryan, A. J.; Bras, W.; Almdal, K.; Mortensen, K. *Macromolecules* **1995**, *28*, 8796−806.
(3) Zhao, J.; Majumdar, B.; Schulz, M. F.; Bates, F. S.; Almdal, K.; Mortensen, K.; Hajduk, D. A.; Gruner, S. M. *Macromolecules* **1996**, *29*, 1204−15.
(4) Bates, F. S.; Fredrickson, G. H. *Phys. Today* **1999**, *52*, 32−38.
(5) Floudas, G.; Vazaiou, B.; Schipper, F.; Ulrich, R.; Wiesner, U.; Iatrou, H.; Hadjichristidis, N. *Macromolecules* **2001**, *34*, 2947−2957.
(6) Davidock, D. A.; Hillmyer, M. A.; Lodge, T. P. *Macromolecules* **2003**, *36*, 4682−4685.
(7) Matsen, M. W.; Bates, F. S. *Macromolecules* **1996**, *29*, 1091−8.
(8) Delacruz, M. O.; Sanchez, I. C. *Macromolecules* **1986**, *19*, 2501−2508.
(9) Hadjichristidis, N.; Iatrou, H.; Behal, S. K.; Chludzinski, J. J.; Disko, M. M.; Garner, R. T.; Liang, K. S.; Lohse, D. J.; Milner, S. T. *Macromolecules* **1993**, *26*, 5812−5815.
(10) Matsen, M. W.; Schick, M. *Macromolecules* **1994**, *27*, 6761−6767.
(11) Milner, S. T. *Macromolecules* **1994**, *27*, 2333−2335.
(12) Auschra, C.; Stadler, R. T. *Macromolecules* **1993**, *26*, 2171−2174.
(13) Mogi, Y.; Nomura, M.; Kotsuji, H.; Ohnishi, K.; Matsushita, Y.; Noda, I. *Macromolecules* **1994**, *27*, 6755−60.
(14) Goldacker, T.; Abetz, V.; Stadler, R.; Erukhimovich, I.; Leibler, L. *Nature (London)* **1999**, *398*, 137−139.
(15) Bailey, T. S.; Pham, H. D.; Bates, F. S. *Macromolecules* **2001**, *34*, 6994−7008.
(16) Bailey, T. S.; Hardy, C. M.; Epps, T. H., III; Bates, F. S. *Macromolecules* **2002**, *35*, 7007−7017.
(17) Epps, T. H., III; Bailey, T. S.; Waletzko, R.; Bates, F. S. *Macromolecules* **2003**, *36*, 2873−2881.
(18) Epps, T. H., III; Cochran, E. W.; Bailey, T. S.; Waletzko, R. S.; Hardy, C. M.; Bates, F. S. *Macromolecules* **2004**, *37*, 8325−8341.
(19) Huckstadt, H.; Gopfert, A.; Abetz, V. *Polymer* **2000**, *41*, 9089−9094.
(20) Avgeropoulos, A.; Paraskeva, S.; Hadjichristidis, N.; Thomas, E. L. *Macromolecules* **2002**, *35*, 4030−4035.
(21) Ludwigs, S.; Boeker, A.; Voronov, A.; Rehse, N.; Magerle, R.; Krausch, G. *Nat. Mater.* **2003**, *2*, 744−747.
(22) Stadler, R. T.; Auschra, C.; Bechmann, J.; Krappe, U.; Voigt-Martin, I.; Leibler, L. *Macromolecules* **1995**, *28*, 3080−3097.
(23) Erukhimovich, I. *Eur. Phys. J. E* **2005**, *18*, 383−406.
(24) Mogi, Y.; Mori, K.; Kotsuji, H.; Matsushita, Y.; Noda, I.; Han, C. C. *Macromolecules* **1993**, *26*, 5169−73.
(25) Erukhimovich, I.; Abetz, V.; Stadler, R. *Macromolecules* **1997**, *30*, 7435−7443.
(26) Brinkmann, S.; Stadler, R.; Thomas, E. L. *Macromolecules* **1998**, *31*, 6566−6572.
(27) Neumann, C.; Loveday, D. R.; Abetz, V.; Stadler, R. *Macromolecules* **1998**, *31*, 2493−2500.
(28) Corte, L.; Yamauchi, K.; Court, F.; Cloitre, M.; Hashimoto, T.; Leibler, L. *Macromolecules* **2003**, *36*, 7695−7706.
(29) Epps, T. H.; III.; Cochran, E. W.; Hardy, C. M.; Bailey, T. S.; Waletzko, R. S.; Bates, F. S. *Macromolecules* **2004**, *37*, 7085−7088.
(30) Leibler, L. *Macromolecules* **1980**, *13*, 1602−17.
(31) Hadjichristidis, N.; Pispas, S.; Floudas, G. A. *Block Copolymers: Synthetic Strategies, Physical Properties, and Applications;* Wiley-Interscience: Hoboken, NJ, 2003.
(32) Rosedale, J. H.; Bates, F. S. *Macromolecules* **1990**, *23*, 2329−38.
(33) Burger, C.; Micha, M. A.; Oestreich, S.; Forster, S.; Antonietti, M. *Europhys. Lett.* **1998**, *42*, 425−429.
(34) Cochran, E. W.; Morse, D. C.; Bates, F. S. *Macromolecules* **2003**, *36*, 782−792.
(35) Mogi, Y.; Mori, K.; Matsushita, Y.; Noda, I. *Macromolecules* **1992**, *25*, 5412−15.
(36) Epps, T. H., III; Bailey, T. S.; Pham, H. D.; Bates, F. S. *Chem. Mater.* **2002**, *14*, 1706−1714.
(37) Fetters, L. J.; Lohse, D. J.; Richter, D.; Witten, T. A.; Zirkel, A. *Macromolecules* **1994**, *27*, 4639−47.
(38) Brandrup, J., Immergut, E. H., Eds. *Polymer Handbook*, 3rd ed.; Wiley: New York, 1989.
(39) Epps, T. H.; III.; Chatterjee, J.; Bates, F. S. *Macromolecules* **2005**, *38*, 8775−8784.
(40) Tyler, C. A.; Morse, D. C. *Phys. Rev. Lett.* **2005**, *94*, 208302.
(41) Park, M. J.; Bang, J.; Harada, T.; Char, K.; Lodge, T. P. *Macromolecules* **2004**, *37*, 9064−9075.
(42) Banaszak, M.; Whitmore, M. D. *Macromolecules* **1992**, *25*, 3406−12.
(43) Laurer, J. H.; Khan, S. A.; Spontak, R. J.; Satkowski, M. M.; Grothaus, J. T.; Smith, S. D.; Lin, J. S. *Langmuir* **1999**, *15*, 7947−7955.
(44) King, M. R.; White, S. A.; Smith, S. D.; Spontak, R. J. *Langmuir* **1999**, *15*, 7886−7889.
(45) Lai, C.; Russel, W. B.; Register, R. A. *Macromolecules* **2002**, *35*, 4044−4049.
(46) Chastek, T. Q.; Lodge, T. P. *Macromolecules* **2003**, *36*, 7672−7680.
(47) Kossuth, M. B.; Morse, D. C.; Bates, F. S. *J. Rheol.* **1999**, *43*, 167−196.
(48) Urbas, A. M.; Maldovan, M.; DeRege, P.; Thomas, E. L. *Adv. Mater. (Weinheim, Ger.)* **2002**, *14*, 1850−1853.
(49) Cavicchi, K. A.; Lodge, T. P. *Macromolecules* **2004**, *37*, 6004−6012.
(50) Cavicchi, K. A.; Lodge, T. P. *Macromolecules* **2003**, *36*, 7158−7164.
(51) Helfand, E.; Wasserman, Z. R. *Macromolecules* **1976**, *9*, 879−88.
(52) Semenov, A. N. *Sov. Phys. JETP* **1985**, *61*, 733.

MA052132O